



Fermi National Accelerator Laboratory

FERMILAB-Conf-98/144-E

D0 and CDF

Inclusive Jet Cross Section at the Tevatron

V.D. Elvira

For the D0 and CDF Collaborations

*State University of New York at Stony Brook
Stony Brook, New York 11794-3800*

*Fermi National Accelerator Laboratory
P.O. Box 500, Batavia, Illinois 60510*

May 1998

Published Proceedings of the *XXXIIIrd Rencontres de Moriond, QCD and High Energy Hadronic Interactions*, Les Arcs, France, March 21-28, 1998

Disclaimer

This report was prepared as an account of work sponsored by an agency of the United States Government. Neither the United States Government nor any agency thereof, nor any of their employees, makes any warranty, expressed or implied, or assumes any legal liability or responsibility for the accuracy, completeness, or usefulness of any information, apparatus, product, or process disclosed, or represents that its use would not infringe privately owned rights. Reference herein to any specific commercial product, process, or service by trade name, trademark, manufacturer, or otherwise, does not necessarily constitute or imply its endorsement, recommendation, or favoring by the United States Government or any agency thereof. The views and opinions of authors expressed herein do not necessarily state or reflect those of the United States Government or any agency thereof.

Distribution

Approved for public release; further dissemination unlimited.

INCLUSIVE JET CROSS SECTION AT THE TEVATRON

V. D. ELVIRA

*Department of Physics**State University of New York at Stony Brook**Stony Brook, New York 11794-3800, USA**e-mail: daniel@fnal.gov**for the DØ and CDF collaborations*

We report preliminary measurements of the central inclusive jet cross section at $\sqrt{s} = 1.8$ TeV by the DØ and the CDF collaborations at the $\bar{p}p$ Fermilab collider. They are based on an integrated luminosity of 92 and 87 pb^{-1} , respectively. The cross sections are measured as a function of jet transverse energy in the pseudorapidity interval $0.1 < |\eta| < 0.7$ (CDF), and the two pseudorapidity ranges $|\eta| < 0.5$ and $0.1 < |\eta| < 0.7$ (DØ). DØ reports good agreement with the Next-to-Leading Order QCD predictions currently available. CDF observes an excess above 200 GeV, which can be accommodated with a modification in the gluon distribution function at high x .

1 Introduction

High transverse momentum jets are predominantly produced in inelastic non-diffractive proton-antiproton collisions by two body scattering of a single proton constituent with an antiproton constituent. Predictions for the inclusive jet cross section have been made^{1,2,3} using Next-to-Leading Order (NLO) Quantum ChromoDynamics (QCD). These calculations reduce theoretical uncertainties to approximately 30%⁴. We measure the inclusive double differential jet cross section, $d^2\sigma/dE_T d\eta$, as a function of the jet E_T , defined as the energy transverse to the incident beams. We use the data samples collected during the period 1994-1995 by the DØ⁵ and CDF⁶ detectors at the Fermilab Tevatron Collider. Previous measurements of inclusive jet production with smaller data sets have been performed and published by the UA2⁷ and CDF⁸ experiments. In particular, the CDF collaboration has reported excess jet production at large E_T relative to the QCD predictions.

2 Sample Selection

Jet detection in the DØ detector primarily utilizes the uranium-liquid argon calorimeters. Pseudorapidity is defined as $\eta = -\ln(\tan(\theta/2))$, where θ is the polar angle of the object relative to the proton beam. The calorimeter depth in units of interaction lengths is on the order of 7.2 for $|\eta| < 0.7$. It is segmented into towers of $\Delta\eta \times \Delta\varphi = 0.1 \times 0.1$, where φ is the azimuthal angle in radians. Online, event selection was performed in two hardware stages and a final software stage. The final stage selected jet candidates using a fast reconstruction algorithm and imposed specified thresholds on the jet E_T . The software jet thresholds were 30, 50, 85, and 115 GeV with integrated luminosities of 0.34, 4.6, 55, and 92 pb^{-1} respectively.

Jets were reconstructed offline using an iterative jet cone algorithm with a cone radius of $\mathcal{R}=0.7$ in η - ϕ space⁹. Background jets from isolated noisy calorimeter cells and accelerator losses were eliminated with quality cuts. Background events from cosmic ray bremsstrahlung or mis-vertexed events were eliminated by cutting on the missing transverse energy in each event,

\cancel{E}_T . Residual background contamination is less than 1% at all $E_T < 500$ GeV based on event simulations with imposed noise distributions and on scanning of all very high E_T jet candidates¹⁰.

CDF calorimeters use lead-scintillator or steel-scintillator/gas as passive and active materials, respectively. The calorimeter depth is on the order of 5.5 interaction lengths for $|\eta| < 0.7$. The segmentation in η - φ space is 0.1 radians \times 15°/5° in the central/forward regions. Event selection is done similarly to DØ. Trigger thresholds of 20, 50, 70, and 100 GeV were imposed to jets. Jets were reconstructed using a cone algorithm¹¹ with radius of $\mathcal{R}=0.7$. Cosmic rays and accelerator loss backgrounds were removed with cuts on event energy timing and on \cancel{E}_T . The remaining backgrounds are estimated to be less than 0.5% in any E_T bin.

3 Energy Corrections

At DØ the jet E_T was corrected for offsets due to the underlying event, additional interactions, and energy depositions from uranium decay; detector uniformity; detector response; and showering loss¹². The showering correction compensates for energy (from particles emitted within the cone) that leaks outside the cone during particle showering inside the calorimeters. The response was derived from γ -jet events using momentum conservation in the transverse plane. At $\eta = 0$, the mean total jet energy correction factor is $1.160 \pm 0.015\%$ at 100 GeV and $1.120 \pm 0.023\%$ at 400 GeV. The steeply falling E_T spectrum is distorted by jet energy resolution. The distortion is corrected by assuming a trial unsmear spectrum $(AE_T^{-B}) \cdot (1 - 2E_T/\sqrt{s})^C$, smearing it with the measured resolution, and comparing the smeared result with the measured cross section. This procedure is repeated by varying the parameters A, B , and C until the observed cross section and smeared trial spectrum are in good agreement. At all E_T the resolution, as measured with dijet E_T balance, is well described by a gaussian distribution; σ at 100 GeV is 7.5%. Resolution correction reduces the observed cross section by $13 \pm 3\%$ ($8 \pm 2\%$) at 60 (400 GeV).

At CDF the measured E_T spectrum is corrected for detector and smearing effects caused by finite E_T resolution with the “unsmearing procedure” described in Ref.¹³. A Monte Carlo simulation was tuned to the CDF data and used to determine the detector response functions. A trial true (unsmear) spectrum was smeared with detector effects and compared to the raw data. The parameters of the trial spectrum were iterated to obtain the best match between the smeared trial spectrum and the raw data. The unsmearing correction may be thought as an E_T correction, on the order of 10%, plus an additional 10% (70%) correction to the cross section at 70 GeV (400 GeV).

Figures 1-2 show the energy scale and unsmearing correction factors for the two experiments. In the case of DØ the point-to-point correlation coefficients of the jet energy response relative to energy values of 20, 50, 100, and 500 GeV are also shown. The response contributes the largest uncertainty to the jet energy scale and, therefore, to the inclusive cross section. The large correlation coefficients translate into low flexibility for the inclusive cross section to a shape change at high E_T .

4 Results

The DØ fully corrected cross section for $|\eta| < 0.5$, shown in Fig. 3, has been averaged over each E_T bin (ΔE_T) and over the central unit of rapidity ($\Delta\eta=1$). Figure 3 (left) also shows a theoretical prediction for the cross section from the NLO event generator JETRAD³. There is good agreement between the prediction and the data over seven orders of magnitude. The NLO calculation requires specification of the renormalization scale (μ), parton distribution function (pdf), and the parton clustering algorithm. For the theoretical predictions shown here $\mu = E_T^{\max}/2$ where E_T^{\max} is the maximum jet E_T in the generated event. In Fig. 3 (left) we used CTEQ3M, one of many possible pdf selections discussed in the Ref.¹⁴. For these calculations,

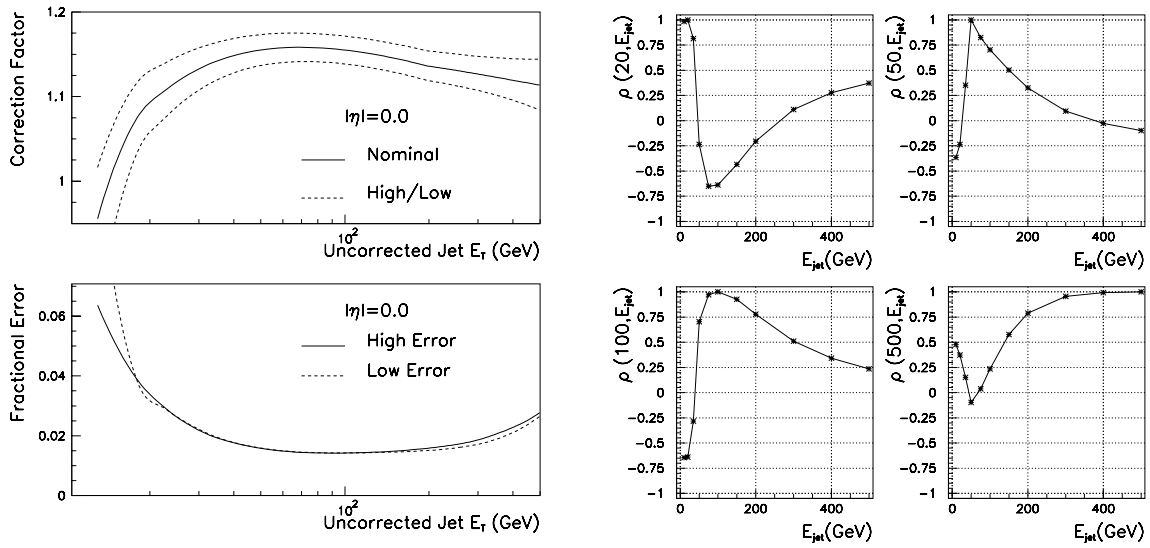


Figure 1: Left: DØ energy scale correction factor and fractional error for $\eta = 0$. Nominal, high (nominal + σ), and low (nominal - σ) correction factors are shown. Right: The four curves show the point-to-point correlation of the DØ response relative to energy values of 20, 50, 100, and 500 GeV respectively.

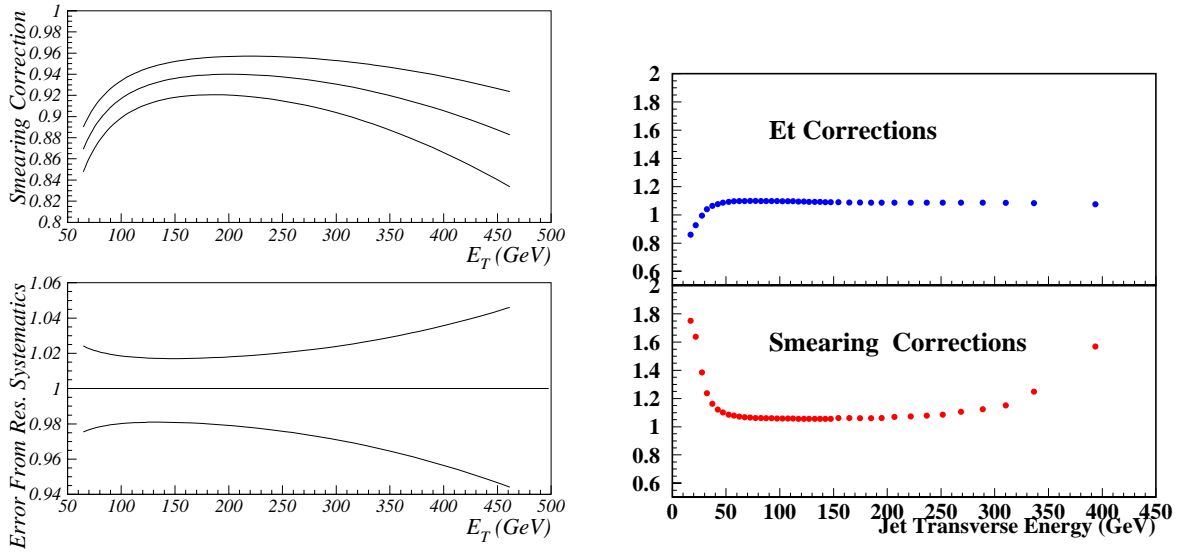


Figure 2: Left: DØ resolution correction and error. Nominal, high (nominal + σ), and low (nominal - σ) correction factors are shown. Right: CDF E_T and smearing correction factors.

partons within $1.3 \mathcal{R}$ of one another were clustered if they were also within $\mathcal{R}=0.7$ of their E_T weighted $\eta-\phi$ centroid. The theoretical choices are fully discussed in Ref.⁴. The errors plotted at each point in Fig. 3 (left) are statistical only and uncorrelated point-to-point in E_T . The data has an overall luminosity error of 6.1%. The band shows the total systematic error (excluding the 6.1% luminosity uncertainty) as a function of E_T . Figure 3 (right) also shows the individual components contributing to the total systematic error. These include jet and event selection, energy scale, resolution unsmearing, trigger matching, and luminosity uncertainties. The components were added in quadrature to obtain the total error. The jet energy scale uncertainty dominates over the whole kinematic range. Errors are fully correlated point-to-point in E_T except for the jet selection, trigger match, and energy scale components.

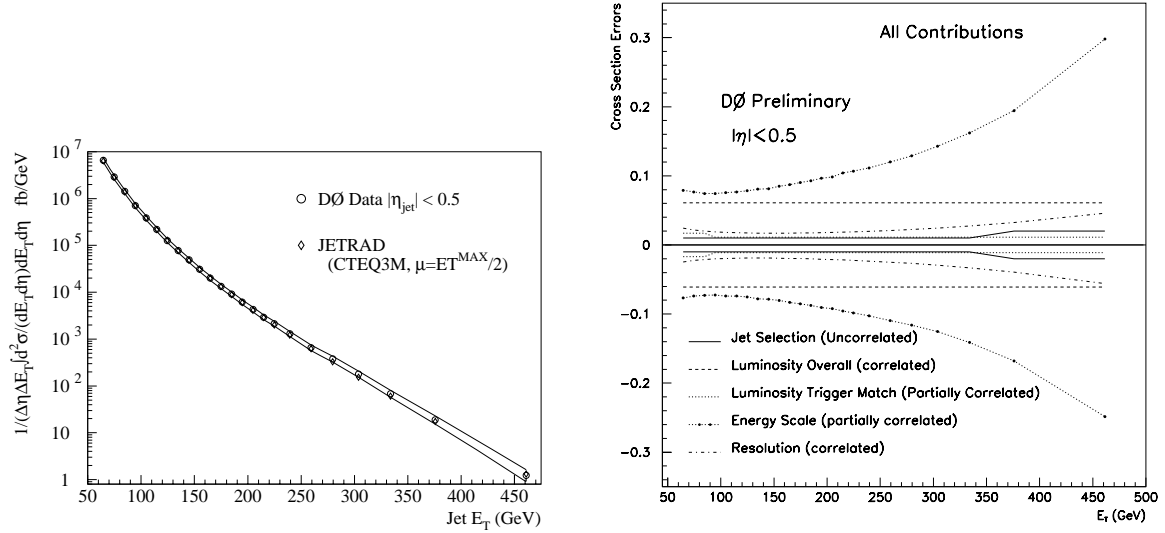


Figure 3: Left: $D\bar{O}$ inclusive jet cross section averaged over the $|\eta| < 0.5$ range. The circles are the data and the diamonds the theoretical prediction. The solid band shows the total systematic error. Right: individual components contributing to the total systematic uncertainty on the inclusive jet cross section measurement. The jet energy scale error dominates; errors are fully correlated point-to-point in E_T except the jet selection, trigger match, and energy scale components.

Figure 4 (left) shows the CDF measurements of $(D-T)/T$ versus jet E_T in the range $0.1 < |\eta| < 0.7$, where D denotes data and T denotes the theoretical prediction. The error bars are statistical only. Figure 4 (left) allows a comparison of the CDF published inclusive jet cross section⁸ (Run 1A in open circles) with the preliminary result using a larger sample (Run 1B in full circles). The two measurements are in good agreement. The theory is NLO QCD (EKS¹), using the CTEQ3M pdf set. The CTEQ3M set was derived from deep inelastic scattering, early data from the electron-proton collider, HERA, and W boson asymmetry and Drell-Yan measurements. The systematic uncertainties of the preliminary measurement are not finalized; they are expected to be similar to published results⁸. The CDF inclusive jet cross section is consistent with NLO QCD predictions below $E_T \sim 200$ GeV. The apparent excess at high E_T can be accommodated with a modification in the gluon distribution function at high x .

Figure 4 (right) shows the $D\bar{O}$ measurements of $(D-T)/T$ plots in two ranges: $|\eta| < 0.5$ and $0.1 < |\eta| < 0.7$. The second measurement has been performed to facilitate the comparison between the data of the two experiments. The theory is JETRAD, using the CTEQ3M pdf set. The error bars are statistical only, and the dashed band shows the total systematic uncertainty in the ratio. The $D\bar{O}$ preliminary result is in good agreement with NLO QCD predictions over the whole measured E_T range. Figure 5 (left) shows $(D-T)/T$ ratios of the $D\bar{O}$ data and the NLO QCD prediction (CTEQ4M). The CTEQ4M pdf set includes recent data from HERA, as well the $D\bar{O}$ (an early version) and CDF preliminary inclusive jet cross sections. The prediction

and the data are in good agreement over the whole measured E_T range.

Figure 5 (right) shows the ratio $(D\emptyset\text{-CDF})/\text{CDF}$, where $D\emptyset$ means $D\emptyset$ preliminary data points and CDF means a fit to the CDF preliminary measurement. The plot shows the $D\emptyset$ systematic uncertainty propagated on the ratio, and also the fractional error on the cross section for both experiments. For CDF the band is the uncertainty taken from the published measurement⁸ and overlapped onto the preliminary result. The difference between the measurements of the two experiments are well within the systematic error bands, below $E_T \sim 300$ GeV. It should be noted that the $D\emptyset$ measurement is expected to be 3.5% lower than CDF's, given that the two experiments use a different value for the $\bar{p}p$ total inelastic cross section in the luminosity determination; CDF uses its own measurement and $D\emptyset$ the world average (CDF and E710 results).

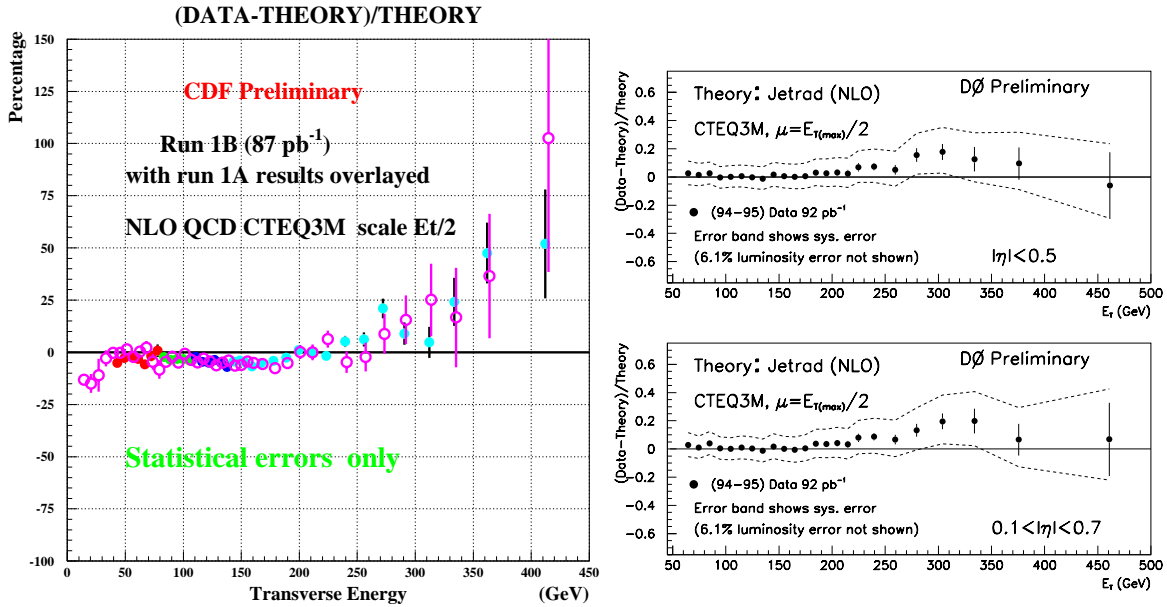


Figure 4: Left: $(D-T)/T$ versus jet E_T (CDF). The theory is NLO QCD (EKS) using $\mu = E_T^{\text{jet}}/2$, and the CTEQ3M pdf set. The open circles show the published measurement (Run 1A) and the full circles show the preliminary measurement in the $0.1 < |\eta| < 0.7$ region using a larger sample (Run 1B). Systematic errors on the preliminary measurement are not finalized. Right: $(D-T)/T$ from $D\emptyset$ in the pseudorapidity ranges, $|\eta| < 0.5$ and $0.1 < |\eta| < 0.7$. The theory is NLO QCD (JETRAD), using CTEQ3M and $\mu = E_T^{\max}/2$. The dashed band is the total systematic uncertainty on the ratio (luminosity error not included).

5 Summary and Conclusions

CDF and $D\emptyset$ have made precise measurements of the inclusive jet cross section. The systematic uncertainties are of the same order as, or smaller than, the uncertainties in the NLO QCD predictions. The $D\emptyset$ preliminary measurement has been improved with respect to the result presented in Ref.¹⁵ (reduced uncertainties and error correlation analysis); it remains in good agreement with NLO QCD predictions. A quantitative comparison between the $D\emptyset$ data and theory is underway. It will be based on a χ^2 test using the total error covariance matrix, which includes correlation information in the non-diagonal elements. The CDF preliminary measurement is consistent with NLO QCD predictions below $E_T \sim 200$ GeV. The apparent excess at high E_T can be accommodated with a modification in the gluon distribution function at high x . The difference between the measurements of the two experiments are well within the error bands, below $E_T \sim 300$ GeV.

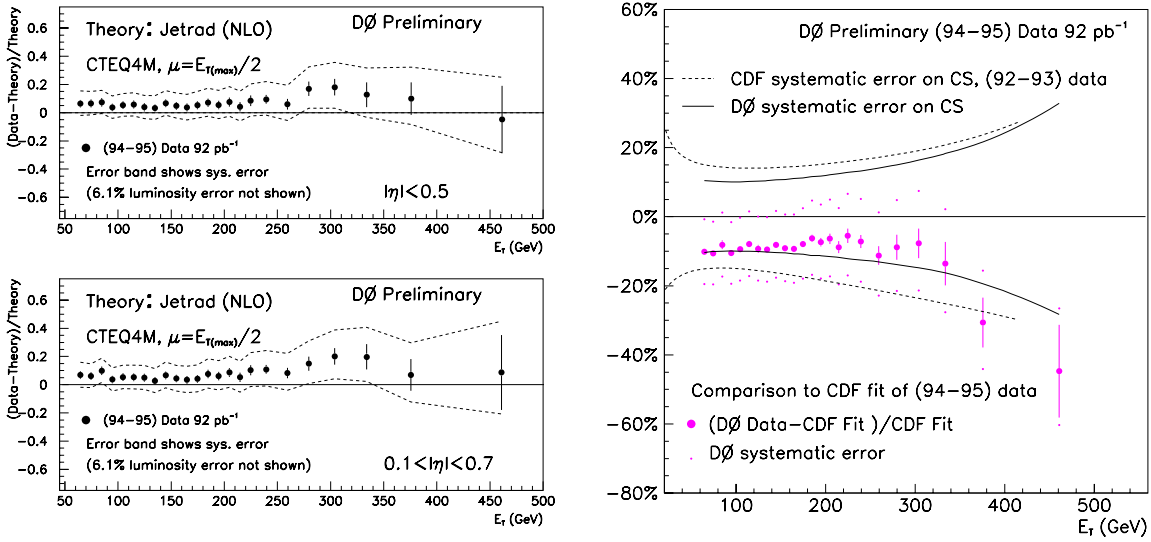


Figure 5: Left: $(D-T)/T$ versus jet E_T ($D\bar{O}$) in the pseudorapidity ranges, $|\eta| < 0.5$ and $0.1 < |\eta| < 0.7$. The theory is NLO QCD (JETRAD) using $\mu = E_T^{\max}/2$, and the CTEQ4M pdf set. The dashed band is the total systematic uncertainty on the ratio (luminosity error not included). Right: Cross section ratio $(D\bar{O}-CDF)/CDF$, where $D\bar{O}$ means $D\bar{O}$ data points and CDF means a fit to the CDF preliminary measurement. The small circles are the $D\bar{O}$ systematic uncertainty propagated on the ratio. The solid and dashed bands are the fractional error on the cross section for $D\bar{O}$ and CDF, respectively. For CDF the band is the uncertainty taken from the published measurement and overlapped onto the preliminary result.

References

1. S. D. Ellis, Z. Kunszt, and D. E. Soper, *Phys. Rev. Lett.* **64**, 2121 (1990).
2. F. Aversa, *et al.*, *Phys. Rev. Lett.* **65**, (1990).
3. W. T. Giele, E. W. N. Glover, and D. A. Kosower, *Phys. Rev. Lett.* **73**, 2019 (1994).
4. B. Abbott *et al.*, Accepted in EPJ C and Hep-Ph/9801285, (1998).
5. S. Abachi *et al.*, (DØ Collaboration), *Nucl. Instrum. Methods A* **338**, 185 (1994).
6. F. Abe *et al.*, (CDF Collaboration), *Nucl. Instrum. Methods A* **271**, 387 (1988).
7. J. Alitti *et al.*, (UA2 Collaboration), *Phys. Lett. B* **257**, 232 (1991); *Z. Phys. C* **49**, 17 (1991).
8. F. Abe *et al.*, (CDF Collaboration), *Phys. Rev. Lett.* **70**, 1376 (1993). F. Abe *et al.*, (CDF Collaboration), *Phys. Rev. Lett.* **77**, 438 (1996).
9. B. Abbott *et al.*, (DØ Collaboration), Fermilab-Pub-97/242-E, (1997).
10. D. Elvira, Ph. D. Thesis, Universidad de Buenos Aires, Buenos Aires, Argentina (1995).
11. F. Abe *et al.*, (CDF Collaboration), *Phys. Rev. D* **45**, 1448 (1992).
12. B. Abbott *et al.*, (DØ Collaboration), submitted to *Nucl. Instrum. Methods A*, Fermilab-Pub-97/330-E, hep-ex/9805009.
13. F. Abe *et al.*, (CDF Collaboration), *Phys. Rev. Lett.* **70**, 1376, (1993).
14. H. L. Lai *et al.*, *Phys. Rev. D* **51**, 4763 (1995).
15. F. Nang for the CDF and DØ Collaborations, Fermilab-Conf-97/192-E. Published in the proceedings of the 32nd Rencontres de Moriond: QCD and High-Energy Hadronic Interactions, Les Arcs, France, 1997, p.185.